Super multi-view three-dimensional display through spatial-spectrum time-multiplexing of planar aligned *OLED* microdisplays

Dongdong Teng, Lilin Liu,* and Biao Wang

State Key Laboratory of Optoelectronic Materials and Technologies, School of Physics and Engineering, Sun Yat-sen University, Guangzhou 510275, China

liullin@mail.sysu.edu.cn

Abstract: Existing super multi-view (*SMV*) technologies depend on ultra-high resolution two-dimensional (*2D*) display panel or large number of *2D* display panels to obtain dense sub-viewing-zones for constructing more natural three-dimensional (*3D*) display by pure spatial-multiplexing. Through gating the spatial-spectrum of each *OLED* microdisplay, the present work proposes a new *SMV* technology combining time- and spatial-multiplexing based on planar-aligned *OLED* microdisplays. The inherent light emission characteristics of *OLED*, i.e. large divergence angle, guarantees a homogeneous light intensity distribution on the spectrum plane, which is a necessary condition for successful time multiplexing. The developed system bears with low requirements on the number of *2D* display panels. The factors influencing the lateral display resolution limit are discussed and the optimum value is deduced. Experimentally, a prototype system with 60 sub-viewing-zones is demonstrated by 12 *OLED* microdisplays. The horizontal interval between adjacent sub-viewing-zones is 1.6*mm*.

OCIS codes: (110.0110) Imaging systems; (120.2040) Displays.

References and links

1. Y. Kajiki, H. Yoshikawa, and T. Honda, "Hologram-like video images by 45-view stereoscopic display," Proc. SPIE **3012**, 154–166 (1997).
2. Y. Kajiki, H. Yoshikawa, and T. Honda, "Ocular accommodation by super multi-view stereogram and 45-view stereoscopic display," Proceedings of the Third International Display Workshops (IDW'96), **2**, 489–492 (1996).
3. Y. Takaki, "Thin-type natural three-dimensional display with 72 directional images," Proc. SPIE **5664**, 56–63 (2005).
4. Y. Takaki, Y. Urano, S. Kashiwada, H. Ando, and K. Nakamura, "Super multi-view windshield display for long-distance image information presentation," Opt. Express **19**(2), 704–716 (2011).
5. H. Nakanuma, H. Kamei, and Y. Takaki, "Natural 3D display with 128 directional images used for human-engineering evaluation," Proc. SPIE **5664**, 28–35 (2005).
6. J. H. Lee, J. Park, D. Nam, S. Y. Choi, D. S. Park, and C. Y. Kim, "Optimal projector configuration design for 300-Mpixel multi-projection 3D display," Opt. Express **21**(22), 26820–26835 (2013).
7. Y. Takaki and N. Nago, "Multi-projection of lenticular displays to construct a 256-view super multi-view display," Opt. Express **18**(9), 8824–8835 (2010).
8. A. R. Travis, "Autostereoscopic 3-D display," Appl. Opt. **29**(29), 4341–4342 (1990).
9. N. A. Dodgson, J. R. Moore, S. R. Lang, G. Martin, and P. Canepa, "A time sequential multi-projector autostereoscopic display," J. SID **8**(2), 169–176 (2000).
10. J. Y. Son, V. V. Smirnov, K. T. Kim, Y. S. Chun, and S.-S. Kim, "A 16-views TV system based on spatial jointing of viewing zones," Proc. SPIE **3957**, 184–190 (2000).
11. T. Kozacki, G. Finke, P. Garbat, W. Zaperty, and M. Kujawińska, "Wide angle holographic display system with spatiotemporal multiplexing," Opt. Express **20**(25), 27473–27481 (2012).
12. J. Y. Son and B. Javidi, "Three-dimensional imaging methods based on multiview images," J. Disp. Technol. **1**(1), 125–140 (2005).
13. Y. Takaki and H. Nakanuma, "Improvement of multiple imaging system used for natural 3D display which generates high-density directional images," Proc. SPIE **5243**, 42–49 (2003).

#220140 - $15.00 USD Received 31 Jul 2014; revised 7 Nov 2014; accepted 12 Nov 2014; published 12 Dec 2014

1. Introduction

Through projecting numerous two-dimensional (*2D*) perspective views of target three-dimensional (*3D*) object to dense sub-viewing-zones, the glasses-free super multi-view (*SMV*) technology [1] can provide *3D* display with smooth motion parallax. Each displayed *3D* spatial spot is formed by superimposing incoherent light beams coming from different *2D* views. The interval between adjacent sub-viewing-zones is set smaller than the pupil diameter of the eye. So, at least two different views are delivered to a single eye pupil and the eyes can focus on the spot. The high-density directional (*HDD*) display is very similar to *SMV*, but the used *2D* views are orthogonal views. The angle pitch must be small enough to satisfy the condition for *SMV* display, that is, at least two different views are delivered to a single eye pupil [2]. To provide binocular disparity and motion parallax simultaneously, a large number of sub-viewing-zones are necessary for constructing a wide viewing zone which could not only accommodate two eyes of a viewer but also provide a proper free space for the movement of the viewer. Up to the present, all the studies on *SMV* or *HDD* do hard to increase the number of sub-viewing-zones by pure spatial-multiplexing, e.g. using display panel with ultra-high resolution [3,4], adopting more display panels [5,6] or both of them [7]. Technologies of this type have a common feature that at least two light beams for one displayed spatial spot pass through the eye pupil simultaneously.

Time-multiplexing is another method for generating multiple sub-viewing-zones where light beams from different *2D* views pass through a displayed spatial spot in a time-sequential manner. In *1990*, *Travis* demonstrated the applicability of time-multiplexing on autostereoscopic *3D* display [8]. A planar multi-switch liquid crystal shutter was placed before a *2D* cathode-ray tube (*CRT*). Different vertical-strip switches of the shutter were gated sequentially and then imaged into different sub-viewing-zones through a Fresnel lens. The *CRT* was refreshed synchronously and rapidly with corresponding *2D* views. Eyes at different sub-viewing-zones could perceive corresponding *2D* views. Based on the persistence of human vision, autostereoscopic display got realized. Subsequently, time-multiplexing of four *CRT*s was implemented for more sub-viewing-zones by *N. A. Dodgson* [9]. They designed a complex lens consisting of *6* element lenses to ensure rays from each pixel of a *CRT* passing through the corresponding "final face". Each *CRT* has a specific "final face", i.e. a rectangular parallel plane where the whole *CRT* is visible to each point on it. In order to spatially superimposing *2D* views projected from different *CRT*s, *CRT*s were aligned in an arc. Therefore, these "final faces" presented different angular offsets between each other. The confliction on occupied physical spaces makes the system accommodate only one planar multi-switch shutter. Thus, if the size of switches was small and multiple *CRT*s were used for *SMV*, some "final faces" presented too great deviations from the multi-switch shutter, making some pixels of the corresponding *CRT*s missed by the switches. So, the system of *N. A. Dodgson* was not extended to *SMV* displays. *J. Y. Son* realized time-multiplexing of two *CRT*s through using a dichronic prism [10], but their system could not accommodate more *CRT*s due to complicated optical structures.

In this letter, employing an array of planar aligned *OLED* microdisplays as display panels, a new *SMV* technology combining the time- and spatial-multiplexing together is proposed. An array of symmetrically and equally spaced apertures is introduced into the spatial-spectrum plane of the microdisplay array. Through an optical structure, all the display panels are imaged into a common *2D* region, but apertures are imaged into different sub-viewing-zones in a time-sequential manner. With different apertures gated sequentially and corresponding perspective views refreshed synchronously, the proposed system can provide enough dense sub-viewing-zones for *SMV*, while bearing with lower requirement on the number of display panels. Different from that in [9], the "final faces" for all *OLED* microdisplays in the proposed system overlap on the planar spatial-spectrum plane. The deviation problem in [9] is avoided. Benefitted from gating the spatial-spectrum, the superimposition of *2D* views becomes precise.

#220140 - $15.00 USD Received 31 Jul 2014; revised 7 Nov 2014; accepted 12 Nov 2014; published 12 Dec 2014

The rest of this paper is organized as follows. In section 2, a spatial-spectrum time-multiplexing technology based on *OLED* microdisplay is explained. Based on the developed time-multiplexing, section 3 describes the *SMV* technology with multiple planar aligned *OLED* microdisplays. Experiments and results are shown in Section 4. Section 5 analyzes the lateral display resolution limit of the proposed system. Section 6 provides conclusions.

2. Time-multiplexing technology based on *OLED* microdisplay

The light emission of an *OLED* pixel presents a large divergence angle. After optical Fourier transformation, the light intensity distribution on the spatial-spectrum plane ($P_{spectrum}$) of an *OLED* microdisplay is approximately homogeneous in the central region, which is a necessary condition to carry out the proposed time-multiplexing technology.

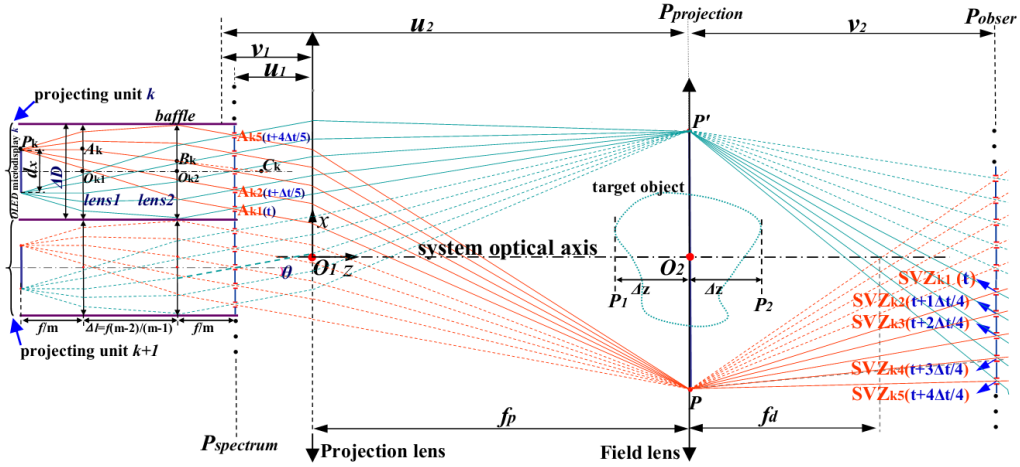

Fig. 1. Optical diagram of the proposed *SMV* system.

An array of symmetrically and equally spaced apertures will be placed on the $P_{spectrum}$ plane of an *OLED* microdisplay *k*, which constructs a projecting unit. Here five apertures (A_{k1}, A_{k2}, A_{k3}, A_{k4} and A_{k5}) with a horizontal interval of $\Delta D/5$ are taken as an example, as shown in Fig. 1. Through a *Projection lens* behind the $P_{spectrum}$ plane, the *OLED* microdisplay *k* is imaged to *PP'* on the focal plane ($P_{projection}$) of the *Projection lens*. A two-step imaging process through the *Projection lens* and a lens (called *Field lens*) located at the $P_{projection}$ plane makes the apertures be imaged onto the observing plane (P_{obser}) as sub-viewing-zones (SVZ_{k1}, SVZ_{k2}, SVZ_{k3}, SVZ_{k4}, SVZ_{k5}). The u_1 and v_1 represent the object distance and image distance of the first imaging. The u_2 and v_2 denote the object distance and image distance of the second imaging. With the apertures being gated sequentially, the *2D* perspective views of the target *3D* object converging to their corresponding sub-viewing-zones are refreshed by the *OLED* microdisplay *k* synchronously. Precisely, at the time *t*, the aperture A_{k1} is gated and other four apertures are closed. A *2D* perspective view converging to the geometrical center of SVZ_{k1} is displayed by the *OLED* microdisplay *k*. Then at $t + \Delta t/5$, A_{k1} is closed and A_{k2} gets opened, synchronously the microdisplay is refreshed with a *2D* perspective view converging to the geometrical center of SVZ_{k2}. And so on, at $t + 2\Delta t/5$, $t + 3\Delta t/5$ and $t + 4\Delta t/5$, A_{k3}, A_{k4} and A_{k5} are gated, respectively. Corresponding *2D* perspective views converging to the geometrical centers of SVZ_{k3}, SVZ_{k4} and SVZ_{k5} are synchronously refreshed by the microdisplay, respectively. Repeating above procedures cyclically, a multi-view display with five sub-viewing-zones gets realized by only one *OLED* microdisplay when the time cycle Δt is small enough for persistence of human vision. Due to the homogeneity of light intensities on the spatial-spectrum plane, the display intensity of each *2D* perspective view is approximately equal when ΔD is not very large.

#220140 - $15.00 USD Received 31 Jul 2014; revised 7 Nov 2014; accepted 12 Nov 2014; published 12 Dec 2014

3. A *SMV* display system with multiple planar aligned *OLED* microdisplays

To obtain more sub-viewing-zones, multiple (N) projecting units are arranged side by side transversely along the system optical axis, as shown in Fig. 1. For simplicity, only two adjacent projecting units are drawn in the figure with sequence number k and $k + 1$. The common optical axis of the *Projection lens* (f_p) and the *Field lens* (f_d) is taken as the optical axis of the display system. Through the public *Projection lens* and *Field lens*, sub-viewing-zones from different projecting units are lined up along the horizontal x-direction on the P_{obser} plane. Benefitted from the adopted optical structure, the projected *2D* views from all planar aligned *OLED* microdisplays are superimposed on the $P_{projection}$ plane precisely, with points P and P' as the common boundary points along the horizontal direction. At each time point, one aperture per projecting unit is gated. For a time cycle consisting of five time points (t, $t + \Delta t/5$, $t + 2\Delta t/5$, $t + 3\Delta t/5$, $t + 4\Delta t/5$), totally $5N$ sub-viewing-zones are obtained. When the sub-viewing-zone interval ($\beta\Delta D/5$) is smaller than the eye pupil diameter, a *SMV* display gets realized by the proposed display system through time-multiplexing of multiple *OLED* microdisplays. Here the $\beta = v_1v_2/u_1u_2$ is the magnification of the sub-viewing-zone to the aperture. The size of the horizontal viewing zone is $\beta N\Delta D$.

In order to make intervals between all adjacent apertures, including those belong to different projecting units, be fixed at $\Delta D/5$, the size of the lens used for Fourier transformation in each projecting unit must be smaller than ΔD, as shown in Fig. 1. At the same time, lights from each pixel on a microdisplay should cover all apertures in the projecting unit so as to make the whole *2D* view be viewable in any sub-viewing-zone. Therefore, a double-lenses (f) structure for Fourier transformation is designed, as shown in Fig. 1. O_{k1} and O_{k2} are the optical centers of the two coaxial lenses (Lens1 and Lens2), respectively. Their optical axis passes through the geometrical center of the microdisplay perpendicularly. The distance between two lenses is $f(m-1)/(m-2)$, where m is a number larger than 2. The normal emission ray from a marginal point pixel (P_k) of the *OLED* microdisplay intersects with the two lenses at A_k and B_k, respectively. C_k is the intersection point between lines A_kB_k and $O_{k1}O_{k2}$. The *OLED* microdisplay has a distance of f/m away from the *Len*1. According to the geometrical relationship shown in Fig. 1, the size of the *Len*2 should be less than ΔD along the horizontal direction. Numerically, the following equation shall be satisfied:

$$\left.\begin{aligned} O_{k2}\mathrm{B}_k < \Delta D/10 \\ \frac{O_{k2}\mathrm{B}_k}{O_{k1}A_k} = \frac{O_{k2}C_k}{O_{k1}C_k} \end{aligned}\right\} \Rightarrow m-1 \geq \frac{5d_x}{\Delta D} \tag{1}$$

where d_x is the horizontal size of the effective working face of the *OLED* microdisplay.

The sequential gating of apertures is implemented through a rotating circular metal plate, called "gating plate" in this paper. The gating plate is placed 2mm behind the $P_{spectrum}$ plane with its rotating axis being parallel with the system optical axis. A pre-designed arc-aperture pattern with an angular pitch of $4.8°$ is enchased into the gating plate, as shown in Fig. 2. Each arc-aperture is with a width of 3mm along the radial direction and covers a central angle of $4°$. An arc-aperture denoted as GA_{kl} is the gating aperture for the aperture A_{kl} on the $P_{spectrum}$ plane. For example, when GA_{11} rotates to the x-axis, the aperture A_{11} gets gated. Here, only a part of the gating plate is shown in Fig. 2(a). Specifically, along the radial direction, 5×2 kinds of arc-apertures are drawn and other $5 \times (N-2)$ kinds of arc-apertures are arranged by the same rule. At a time point, N apertures from N projection units are gated simultaneously. Along the angular direction, a fan-structure with a central angle $24°$ is taken as a unit, as schematically drawn in Fig. 2. Totally there are 15 identical units constructing the circular gating plate. The arc gating apertures ensure that all apertures on the $P_{spetrum}$ plane have an equal gating time wherever their locations on the gating plate are. The gating plate rotates at a constant speed of one cycle per second. The gating time is 11ms and the display frequency of the *3D* image is 15Hz.

#220140 - $15.00 USD Received 31 Jul 2014; revised 7 Nov 2014; accepted 12 Nov 2014; published 12 Dec 2014

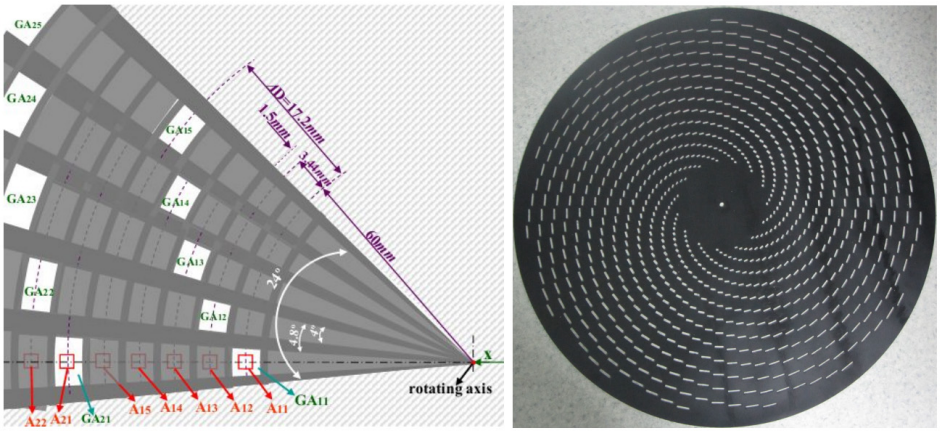

Fig. 2. (a) The schematic drawing of a part of the gating plate with arc-apertures; (b) Photo of the gating plate.

4. Experiments and results

A display system is set up to implement the idea described above. N = 12 white *OLED* microdisplays, with a display area $d_x \times d_y = 7.56 \times 10.08 mm^2$ and a resolution 600×800, from *Yunnan North OLEiD Opto-Electronic Technology Co of China* are used. Their shorter sides are set along the horizontal direction. But each microdisplay is integrated with a control chip on a printed circuit board. The total size of the module is $17mm \times 22mm$. So, ΔD is set as $17.2mm$ in our experiment. The frame rate of the used microdisplay is $75Hz$. To avoid obvious flicking, five time-points are adopted for time-multiplexing and the display frequency is set as $15Hz$ in the prototype system. Although slight flicker is observed in the experiment, this value is enough for the sense of motion. *OLED* has a response time at the scale of μs, exhibiting great potentials to manufacture *OLED* microdisplays with very high frame rates. Once high-speed *OLED* microdisplays are available, higher displaying frequency will come true en route our system. According to Eq. (1), m = 4 is adopted, *Lens*1 ($f = 60mm$) and *Lens*2 ($f = 60mm$) are processed into rectangular shape ($17mm \times 22mm$). Each projecting unit is packaged into a cuboid structure with a frame size of 17.2 $mm \times 24\ mm \times 78mm$ ($W \times H \times L$). The internal structure of an assembled projecting unit is shown in Fig. 3. The baffles ($0.1mm$ thick) shown in Fig. 1, as parts of the cuboid structure, have low reflectivity for light blocking. Five apertures are engraved into a light-blocking membrane. The membrane is braced by an optical glass sheet with five windows which are a little larger than the apertures to guarantee free path for the valuable light rays.

#220140 - $15.00 USD Received 31 Jul 2014; revised 7 Nov 2014; accepted 12 Nov 2014; published 12 Dec 2014

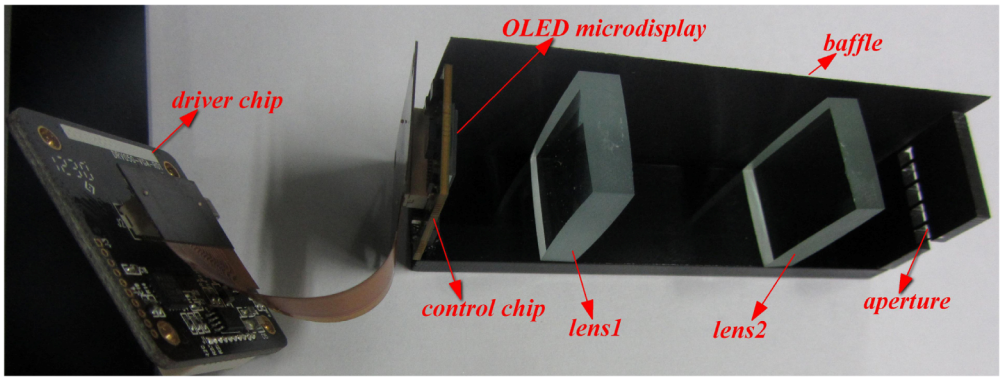

Fig. 3. Photo showing the internal structure of a projecting unit (with the upper package and a baffle removed for photograph).

All lenses in our system are achromatic lens. A Fresnel lens with an aperture of 279.4*mm* × 279.4*mm* from *Edmund Optics* of *America* is taken as the *Projection lens* and a doublet lens with a diameter of 100*mm* is employed as the *Field lens*. The problem of wavefront aberration and chromatic aberration accompanying the usage of the Fresnel lens will be discussed in the following section 5. Figure 4 shows the photograph of the experimental display system. Other system parameters include $f_p = 609.6mm$, $f_d = 200mm$, $u_1 = 60mm$ and $\delta = 2.7mm$. δ is the side length of the quadrate aperture. Under this condition, $\beta = 0.4659$, $v_2 = 284mm$, and the available horizontal display size $PP' = 102mm$. Limited by the physical size of the used field lens, the display space of the target *3D* object is set to be 60*mm* × 60*mm* × 60*mm* in between plane P_1 and P_2 of Fig. 1. The planes P_1 and P_2 have an equal distance, $\Delta z = 30mm$, to the $P_{projection}$ plane. The horizontal viewing zone constructed by 60 sub-viewing-zones is 96.0*mm* which is 1.5 times as large as the average interocular distance (64*mm*) of a viewer. The horizontal interval between adjacent sub-viewing-zones (with a size of 1.26*mm* × 1.26*mm*) is 1.60*mm*. For a pupil of 5*mm*, *i.e.* the average diameter, at least two adjacent sub-viewing-zones can be captured. So the *SMV* effect keeps being active throughout the entire viewing zone along the P_{obser}. In the experiment, a research-type charge coupled device (*CCD*, *SenSys 1602E* from *PM* of America) with an objective aperture of 5*mm* is used to capture images displayed by the prototype display system [11]. The *CCD* can move in the P_{observ} horizontally. Actually, under normal room brightness, the pupil size of human eyes is 3*mm* [12]. Under this condition, two adjacent sub-viewing-zone can be captured entirely only when the eye is centered on the boundary between them. Once the eye deviating from the boundary, only one sub-viewing-zone can be captured entirely, which is accompanied by two partial sub-viewing-zones. Intensities of different perspective views captured by one eye are not balanced. i.e. one view is brighter than the others, resulting in *SMV* effect weakening. More dense sub-viewing-zones are needed to achieve uniform *SMV* effect in the proposed system for viewers with small size pupils. Adopting *OLED* microdisplays with higher frame rates or smaller mechanical sizes can realize this goal, which will be done in the future work.

#220140 - $15.00 USD Received 31 Jul 2014; revised 7 Nov 2014; accepted 12 Nov 2014; published 12 Dec 2014

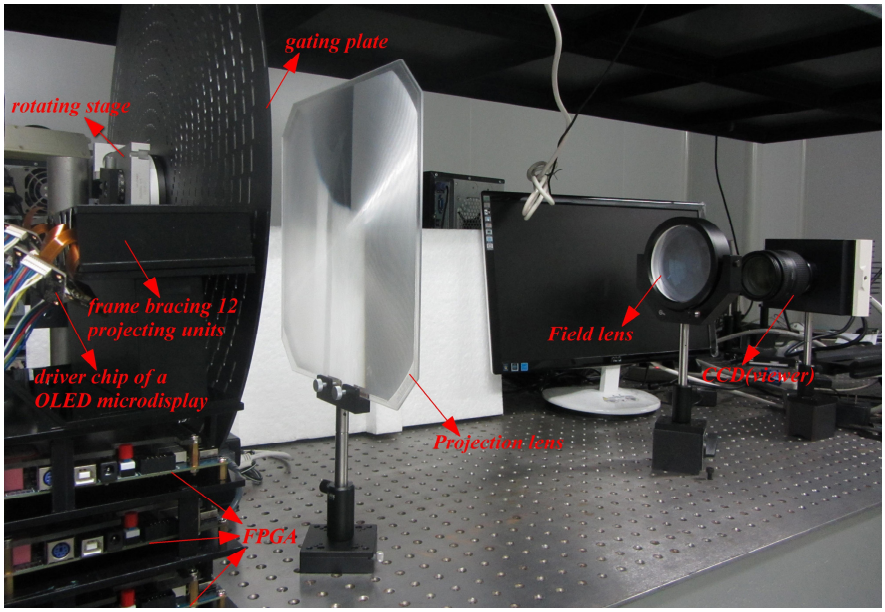

Fig. 4. Photograph of the experimental display system.

A uniform light intensity distribution on the $P_{spectrum}$ plane is a necessary condition for successful time multiplexing. The inherent light emission characteristics of *OLED*, i.e. large divergence angle, guarantees this point. The light intensity distribution on the $P_{spectrum}$ plane is measured through a luminance meter *CS-2000A* from *Konicaminolta*. The measured values at the five apertures of a projection unit are 129.8, 130.4, 131.130.2 and 129.6cd/m^2, confirming a nearly homogeneous light distribution on the $P_{spectrum}$ plane. So the display intensities of different *2D* perspective views are roughly even. The fused *3D* image through superimposing incoherent lights is free from intensity fluctuation for a moving eye.

To verify the capability of focusing on *3D* images produced by the prototype system, two horizontal lines with a spacing of 40*mm* along the optical axis are displayed. The line-width is 0.6*mm*. When the aforementioned *CCD* is focused on one line along the optical axis, the other line becomes blurred due to out-of-focus, as show in Fig. 5. The results reveal that the prototype system is able to produce *3D* images on which the human eye can focus.

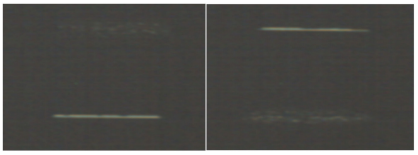

Fig. 5. Captured images when the two lines are on focus separately.

Two 3D objects, i.e. pyramid&teapot and a pelvis, are displayed to demonstrate the proposed idea and system. The captured images with the aforementioned *CCD* being at different positions along the P_{observ} horizontally are shown in Fig. 6.

#220140 - $15.00 USD Received 31 Jul 2014; revised 7 Nov 2014; accepted 12 Nov 2014; published 12 Dec 2014

Fig. 6. Captured images by the *CCD* located at a series of points along the P_{observ} horizontally with a spatial interval of 19*mm* when the proposed display system work.

5. Discussions on the display resolution limit

The size of apertures, i.e. the δ, is a key parameter. As a diffraction-limited incoherent imaging system, the optical transmission function is $tri(\lambda f_p f_x / \delta)$ when the *OLED* microdisplays are imaged onto the $P_{projection}$ plane, where f_x is the spatial frequency. Using the center wavelength (585*nm*) of the *OLED* spectrum for calculation, the displayed resoluble light spot on the $P_{projection}$ plane is $\varepsilon_d = (0.32/\delta)mm$. In the *SMV* system, the displayed *3D* image presented to the viewer is a set of spatial light spots, which are formed by superimposing incoherent cone-shaped light beams coming from different *2D* perspective views. These light spots can be categorized as locating on a series of virtual *2D* display planes, which are parallel with the $P_{projection}$ plane. The lateral size of a displayed light spot on the corresponding virtual display plane depends on the projection size of the cone-shaped beam. For such a diffraction-limited imaging system, the cone-shaped beam has a minimum projection size on the $P_{projection}$ plane and keeps expanding as it leaves away from the $P_{projection}$ plane, no matter along the forward direction or the reverse direction. As shown in Fig. 7, the cone-shaped beam is marked by a pink shadow zone. On the planes (P_1 and P_2) farthest away from the $P_{projection}$ plane, the projection sizes of the cone-shaped beam will have two extremum values. The larger one is taken as the lateral resolution limit of the proposed display system. Based on geometrical optics approximation, the cone-shaped beam can be approximated by a straight-edge beam, constructed by all rays passing through both SVZ_m zone and Q_1Q_2 zone. In the horizontal plane, its distribution zone is between polygonal lines $S_1Q_1M_1$ and $S_2Q_2M_2$, as shown in Fig. 7. Here Q_1 and Q_2 are the boundary points of the projected light spot on the $P_{projection}$ plane. M_1 and M_2 are the boundary points of the SVZ_m. S_1 and S_2 are the intersection points of lines M_2Q_1 and M_1Q_2 with the plane P_1. T_1 and T_2 are the intersection points of lines M_1Q_1 and M_2Q_2 with the plane P_2. Therefore, S_1S_2 and T_1T_2 can be approximated as the displayed light spots on the P_1 plane and P_2 plane, respectively. Their lateral sizes, ε_1 and ε_2, are deduced geometrically by:

#220140 - $15.00 USD Received 31 Jul 2014; revised 7 Nov 2014; accepted 12 Nov 2014; published 12 Dec 2014

$$\begin{cases} \dfrac{\varepsilon_d}{\beta\delta} = \dfrac{z_{c1}}{v_2 - z_{c1}} = \dfrac{z_{c2}}{v_2 + z_{c2}} \\ \dfrac{\varepsilon_1}{\beta\delta} = \dfrac{\Delta z + z_{c1}}{v_2 - z_{c1}} \\ \dfrac{\varepsilon_2}{\beta\delta} = \dfrac{\Delta z + z_{c2}}{v_2 + z_{c2}} \end{cases} \tag{2}$$

$$\Rightarrow \begin{cases} \varepsilon_1 = \dfrac{\Delta z(\beta\delta + \varepsilon_d) + \varepsilon_d v_2}{v_2(\beta\delta + \varepsilon_d) - \varepsilon_d v_2}\beta\delta \\ \varepsilon_2 = \dfrac{\Delta z(\beta\delta - \varepsilon_d) + \varepsilon_d v_2}{v_2(\beta\delta - \varepsilon_d) + \varepsilon_d v_2}\beta\delta \end{cases}$$

where z_{c1} and z_{c2} denote the distances of I_1 and I_2 away from the $P_{projection}$. I_1 is the intersection point of lines M_1Q_2 and M_2Q_1. I_2 is the intersection point of lines M_1Q_1 and M_2Q_2. The larger one of ε_1 and ε_2 represents the lateral resolution limit of the display system.

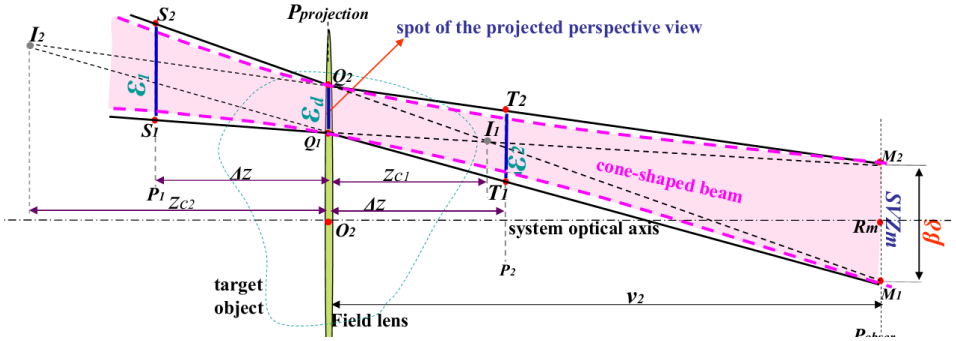

Fig. 7. Geometrical diagram showing the displayed spot sizes of the 2D display planes in the 3D display space.

According to Eq. (2), trade-off between the resolution limit of the $P_{projection}$ plane ($0.32/\delta$) and the size of sub-viewing-zone ($\beta\delta$) leads to an optimum resolution limit. Figure 8 presents the evolution of ε_1 and ε_2 with the aperture size. An optimum lateral resolution limit of 0.2639mm is obtained at δ = 2.7mm. In the experiment, the aperture size is set as 2.7mm × 2.7mm. The *2D* image projected from an *OLED* microdisplay consists of 200 × 200 spots displayed by 352 × 352 effective pixels (i.e. $600\times60/102$), which corresponds to a reachable lateral display resolution of 0.3 mm × 0.3mm.

#220140 - $15.00 USD Received 31 Jul 2014; revised 7 Nov 2014; accepted 12 Nov 2014; published 12 Dec 2014

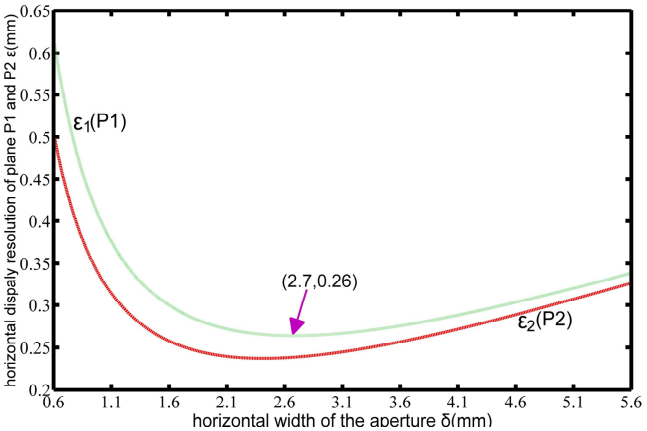

Fig. 8. The evolution of resolution limits of P_1 and P_2 planes with the aperture size.

In the present work, only one row of microdisplays is employed and a horizontal parallax only (HPO) display is demonstrated. When high-speed *OLED* microdisplays are available, equal spaced apertures along the vertical direction can be added and gated in conjunction with multiple rows of projecting units to implement a full parallax 3D display by our system.

To accommodate 12 *OLED* microdisplays, a Fresnel lens with a large size is taken as the *Projection lens* in the proposed system. Since only the central 75% of the aperture of the Fresnel lens gets utilized, the wavefront aberration and the chromatic aberration accompanying the usage of the Fresnel lens do not degrade the image quality obviously in the present experiment. When more *OLED* microdisplays are employed, this kind of degradation must be taken into account. The methods for alleviating the induced image distortion discussed in [13] shall be employed.

6. Conclusions

In conclusion, through spatial-spectrum time-multiplexing of a planar array of 12 *OLED* microdisplays, 60 sub-viewing-zones for one *3D* object are obtained. The interval between adjacent sub-viewing-zones is 1.6*mm* and a *SMV* display gets realized. The influence of the aperture size on the display resolution limit is discussed. An optimum lateral resolution limit of 0.2639*mm* is obtained. The horizontal viewing zone reaches 96*mm* which is about 1.5 times as large as the average interocular distance (64*mm*) of the viewers.

Acknowledgments

The authors gratefully acknowledge support by the Natural Science Foundation of China, Grant No.10802101, and the National High Technology Research and Development Program of China (No.2013AA03A106).

#220140 - $15.00 USD Received 31 Jul 2014; revised 7 Nov 2014; accepted 12 Nov 2014; published 12 Dec 2014